Ultra-Broadband Tunable External Cavity Quantum Well Lasers

D. Mehuys, L. Eng, M. Mittelstein,
T.R. Chen, and A. Yariv

Department of Applied Physics
California Institute of Technology
Pasadena, CA 91125

Abstract

The spectral tunability of properly designed quantum well lasers is demonstrated to equal the range of dye lasers. Theoretical and measured gain spectra are presented to support this statement, and stepwise wavelength tuning over a 125 nm span in GaAs/AlGaAs lasers and 175 nm in InGaAs/AlGaAs lasers are shown.

Introduction

Semiconductor lasers are, in principle, widely tunable sources of radiation because of the breadth of their gain spectrum [1-4]. Since radiative recombination occurs between the conduction and the valence *bands*, rather than between discrete levels, population inversion can be achieved over a broad continuous range of energy whose width scales with the electrical or optical pump level. Furthermore, with the advent of quantum well heterostructure technology, broad gain bandwidths are achieved at a low current cost.

Figure 1 illustrates gain spectra (solid lines) and unbroadened joint density of states spectra (dashed lines) for the two cases of a double heterostructure (DH) and a quantum well (QW) heterostructure laser. The ordinate gives modal gain γ in units of cm^{-1} while the abscissa is photon energy E in units of eV above the 1.42 eV GaAs band gap. While the "bulk" gain $g(E)$ per charge carrier is comparable in DH and QWH lasers, the modal gains $\gamma = \Gamma g(E)$ differ by an order of magnitude because of the disparity in transverse optical confinement factor Γ: typically $\Gamma_{QWH} \simeq 0.1 \times \Gamma_{DH}$. This disparity is illustrated by the dashed lines of Figure 1, which detail the maximum modal gain (upper) and loss (lower) achieved with infinite and zero pump current, respectively. While the maximum modal gain γ_0 obtained per quantized state-quantum well is far less than for the DH laser, at $\gamma_0 \simeq 60-120$ cm^{-1} it is sufficient to overcome the losses of most Fabry-Perot resonators. A key feature of QWH lasers is that, within the QW (i.e., for $E_1 < E < E_0$) the unpumped modal loss is an order of magnitude smaller than for DH lasers. This loss reduction has two important consequences:

(i) To achieve a *given* modal gain $\gamma << \gamma_0$, far less current density is required of QWH than of DH lasers, because proportionately fewer carriers are wasted in pumping the active region to transparency.

(ii) For *equivalent* injected current densities, the QWH laser has a much broader gain bandwidth: the reduced volumetric density of states pushes the quasi-Fermi energies further apart with increased pump level than for DH lasers, providing flat gain over a broad energy range. Gain curve (b) for the QWH laser in Figure 1 is fully a factor of 5 broader than the DH curve. Furthermore, since the spectral gain between the onset energies E_1 of the $n = 1$ quantized state and E_2 of the $n = 2$ quantized state is limited to γ_0, flat gain spectra are obtained at higher pumping levels. This unique property of QWH lasers is exploited for ultra-broadband (> 100 nm) tunability [5-7].

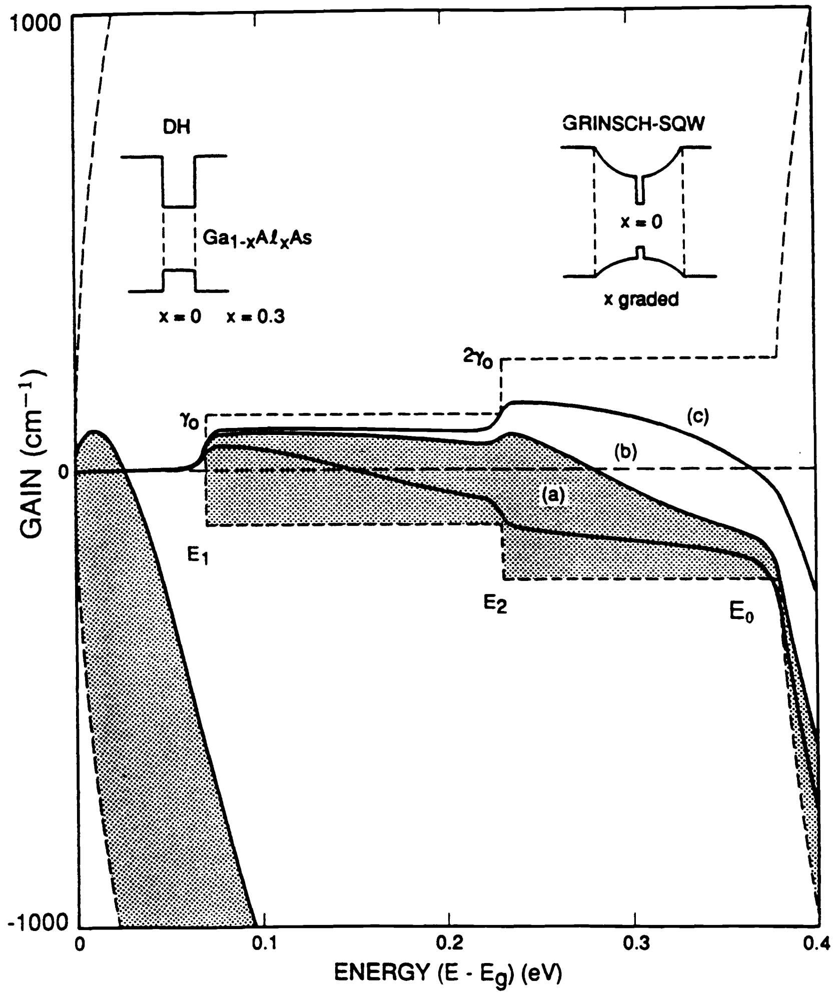

Figure 1. Gain spectra (solid lines) and density of states (dashed lines) for DH and QWH lasers. Curve (b) for the QWH and the DH gain curve correspond to roughly 1.5 kA/cm^2 of current pumping. The gain bandwidth of the QWH laser is 5× as great.

Experiment in GaAs/GaAlAs

The apparatus used in our experiments is shown schematically in Figure 2. The external cavity consists of a collimating lens and a bulk diffraction grating that together image a spectrally resolved, spatially inverted near field back onto the rear facet of a Fabry-Perot semiconductor laser. Only the wavelength of a single longitudinal mode, at $\lambda = \lambda_0$, is refocussed onto the transverse waveguide. Thus, the grating provides an enhanced rear-facet reflectivity at $\lambda = \lambda_0$, which is manifest as a lower threshold current.

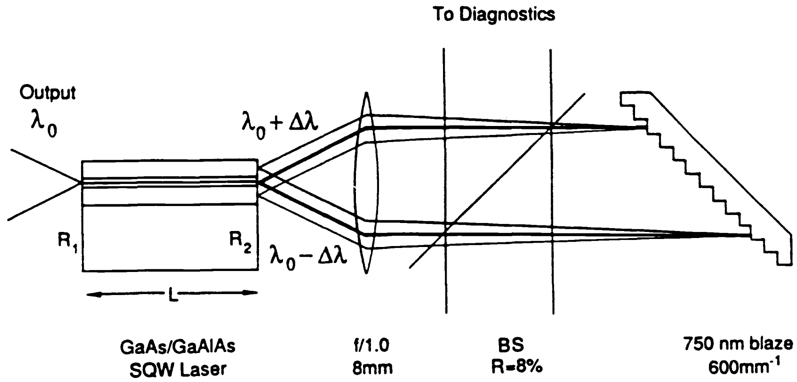

Figure 2. External cavity apparatus.

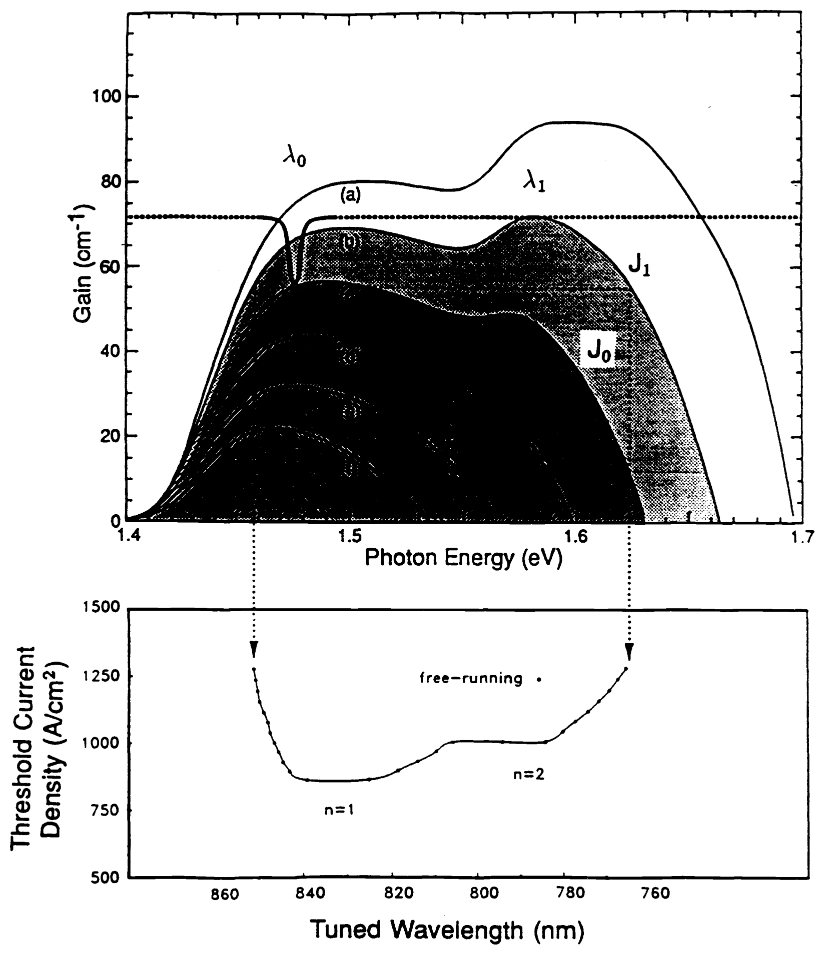

Figure 3.. Computed gain spectra at increasing pump levels for a single QWH laser. The grating-coupled loss curve intersects the gain spectrum at $\lambda = \lambda_0$, giving rise to the threshold current vs. tuned wavelength curve below.

The schematic dependence on photon energy of the grating-coupled external resonator loss is shown in Figure 3, superimposed on a detailed numerical calculation of the QWH laser gain (parameterized by pump current) near the onset of $n = 2$ lasing. With the grating blocked, the loss curve intersects the gain curve (b) (corresponding to current density J_1) at a wavelength $\lambda = \lambda_1$. The local maximum exhibited by the gain at the short wavelength $\lambda = \lambda_1$ is due to the onset of $n = 2$ quantized state contributions at elevated pump levels. With the grating coupled to the Fabry-Perot resonator, the loss level is reduced at the retroreflected wavelength λ_0, because of constructive interference of the reflection from the external cavity with the regular rear-facet reflection. As a result, the loss curve intersects a *different* gain spectrum, curve (c), which is consistent with a lower curent density $J_0 < J_1$. In general, the threshold current in tuned operation is a function of photon energy; it has been estimated theoretically and is shown in the lower half of Figure 3. Note that the curve is skewed so that the lowest threshold currents appear on the long-wavelength side of the spectrum.

From Figure 3 it is evident that a minimum variation in threshold curent density over the tuned energy range can be achieved by designing the resonator losses so as to intersect a flattened gain spectrum. One such spectrum is shown in curve (b), where contributions from just above both the $n = 1$ and $n = 2$ electron-heavy hole (solid lines) and electron-light hole (dashed lines) quantized state transitions are of nearly equal height. As the QW is narrowed, the energy separation of these two peaks increases, leading to a broader tuning range. For a 60 ÅQW, the tuning range is predicted to exceed 100 nm.

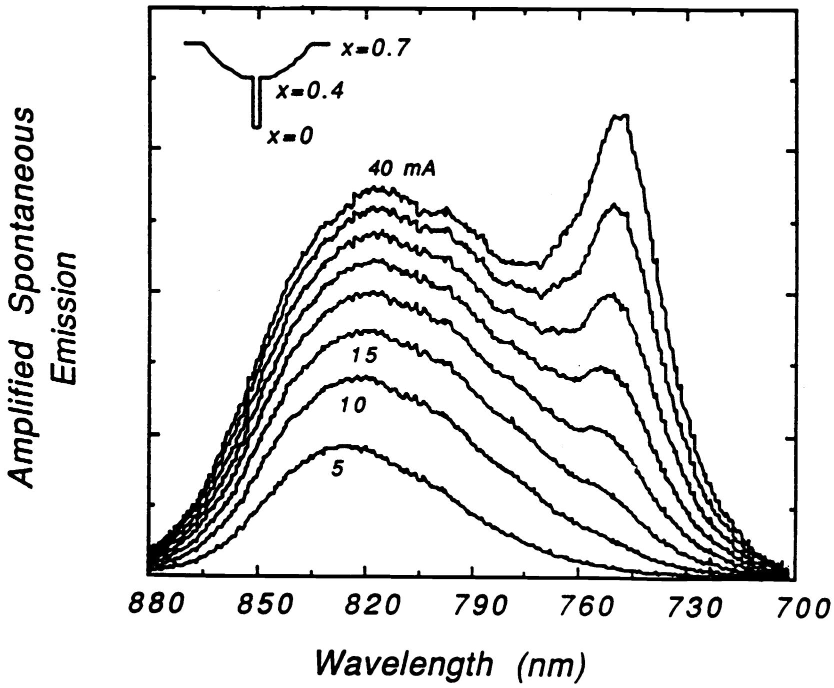

Figure 4. Measured ASE spectra of a narow QW (60 Å) GaAs/AlGaAs stripe laser.

The qualitative features of the gain spectra of Figure 3 were verified by observation of the spectrally resolved amplified spontaneous emission (ASE) of GaAs/GaAlAs lasers. Figure 4 illustrates the measured ASE spectrum at various current levels below threshold for a short ($L = 120\mu$m), narrow stripe ($W = 10\mu$m) laser. The transverse structure consisted of a 60 ÅGaAs QW embedded in a graded ($x = 0.4 \rightarrow 0.7$)Al_xGa$_{1-x}$As separate confinement heterostructure. The emergence of a second peak at short wavelength, $\lambda \simeq 750nm$, with increased pumping signifies participation of the $n = 2$ transition.

For the tuning experiments, lasers were either cleaved short or had antireflection coatings applied in order to achieve the elevated loss level required to access the flattened gain spectrum. The lasers were then coupled to the external cavity: the grating was tuned to successive longitudinal modes of the Fabry-Perot resonator, and the threshold current measured as a function of tuned wavelength. Figure 5 shows the measured tuning characteristic of the same 120 μm-long stripe laser used for the ASE measurements. The 125 nm span, measured under low duty-cycle pulsed conditions, represents a 15.7% tuning range about the center wavelength of $\simeq$ 800 nm. Allowing for current spreading, each 25 mA of current corresponds to approximately 1 kA/cm^2 of injected current density. While these current densities are relatively high, they are not high enough to prohibit CW operation.

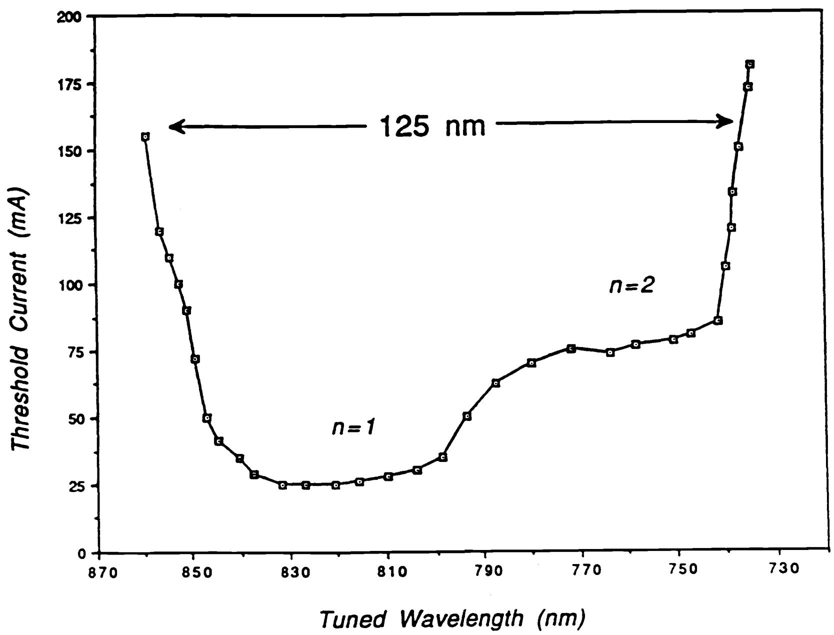

Figure 5. Threshold current vs. tuned wavelength for a narrow QW (60 Åwide) GaAs/AlGaAs stripe laser.

Figure 6 shows the tuning characteristic of an antireflection-coated buried heterostructure laser operated with pulsed current (solid line) and with direct current (dashed line). For CW operation, the laser was mounted p-side up onto a copper heat sink, and water-cooled to maintain near room-temperature operation. As is evident from the plot, the CW characteristic reproduces 95% of the 95 nm pulsed characteristic, with only slightly higher threshold currents. Furthermore, high-resolution spectroscopy of the laser output with a scanning Fabry-Perot interferometer revealed the CW linewidth to be less than the 7.5 MHz resolution limit of the instrument.

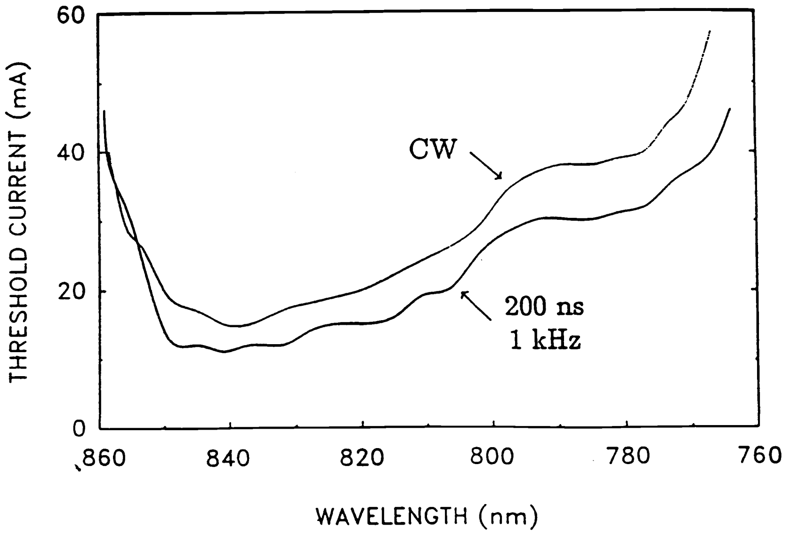

Figure 6. CW and pulsed tuning characteristics of single-mode BH lasers.

Experiment in InGaAs/AlGaAs

Tunable semiconductor laser sources are potential rivals to dye lasers provided that (i) reasonably high power can be attained with good spatial and temporal coherence properties, and (ii) the center wavelength can be varied. Changing the center wavelength via modification of the composition of the active layer heterostructrue is an effective way to realize strong wavelength shifts, and is analagous to changing the dye in dye lasers. For example, lasers with GaInP active regions lase at $\lambda \simeq 680$ nm, while those with InGaAsP active regions lase up to $\lambda \simeq 1650$ nm. In this section, our efforts to tune InGaAs/AlGaAs QWH lasers in the near-1 μm range are reported. Such lasers have potentially important optoelectronic applications since the lasing wavelength, being slightly longer than that of GaAs/AlGaAs structures, see transparent GaAs substrates.

Unlike GaAs/AlGaAs QWH lasers, InGaAs/AlGaAs lasers are not lattice-matched. If the active region thickness does not exceed a critical value (which depends upon the In content of the layer), then the lattice mismatch is accomodated by strain in the QW, causing the InGaAs to undergo biaxial compression [8]. In principle, broadband tunability depends only upon QWH physics, not on the material system, and should therefore be possible in material systems other than AlGaAs. In practice, however, the difficulty in growing non-lattice-matched material of good crystalline quality, and the increased participation of non-radiative recombination processes (such as Auger) at wavelengths longer than $\simeq 1\mu$m imply that extension to other material systems is not certain.

Recently, however, high-quality QWH lasers in InGaAs/AlGaAs have been grown by MBE and MOCVD. Threshold current densities as low as $\simeq 115$ A/cm^2 have led to sub-milliampere threshold currents for coated buried heterostructure lasers [9] and high power (3 W) gain-guided laser arrays [10]. Subsequently, tuning experiments were conducted with 10-μm-wide oxide-isolated stripe lasers of various lengths fabricated from the same material. Figure 7 shows the threshold current as a function of tuned wavelength for a strained $In_{0.2}Ga_{0.8}As$/AlGaAs laser (MBE 912) of length $L = 265\mu$m, as compared with the unstrained GaAs/AlGaAs laser (MBE 881) of Figure 5. The wavelength span of $\simeq 175\mu$m (centered near 920 nm) niceley complements the 125 nm span of the GaAs device (centered near 800 nm) , so that together nearly 300 nm in the near infrared is accessed. In addition, the threshold current densities required for the two material systems are comparable.

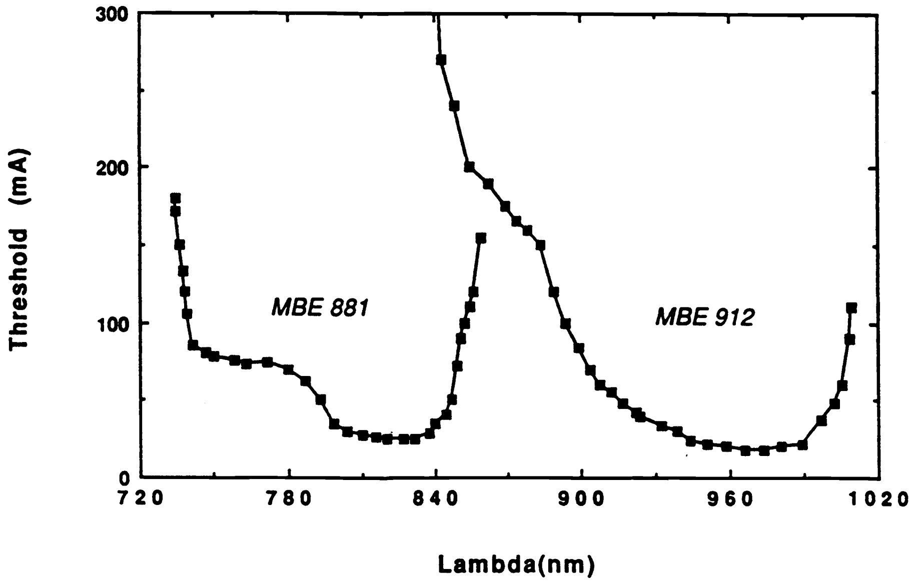

Figure 7. Tuning characteristics of 10 μm stripe InGaAs/AlGaAs lasers (MBE 912) vs. GaAs/AlGaAs lasers (MBE 881).

Conclusions

In conclusion, we have demonstrated stepwise tuning of Fabry-Perot single QWH semiconductor lasers over ranges approaching those of dye lasers. Uncoated GaAs/AlGaAs stripe lasers have been tuned over 125 nm under pulsed operation. Similar tuning of antireflection-coated buried heterostructure lasers over 95 nm under both pulsed and CW operation reveals only a minor increase in threshold in the latter case. Uncoated InGaAs/AlGaAs stripe lasers have been tuned over 175 nm under pulsed operation. The tuning curves for these strained-layer devices are characterized by a greater variation in threshold current over the ultra-broad tuning range when compared with their unstrained counterparts.

References

[1] J.E. Epler, N. Holonyak, Jr., R.D. Burnham, C. Lindstrom, W. Streifer, and T.L. Paoli, "Broadband tuning ($\Delta E \simeq 100\, meV$) of $Al_xGa_{1-x}As$ quantum well heterostructure lasers with an external grating," *Appl. Phys. Lett.* **43**, 740-742 (1983).

[2] J.E. Epler, G.S. Jackson, N. Holonyak, Jr., R.L. Thornton, R.D. Burnham, and T.L. Paoli, "Broadband operation of coupled-stripe multiple quantum well AlGaAs laser diodes," *Appl. Phys. Lett.* **47**, 779-780 (1985).

[3] R. Wyatt, K.H. Cameron, and M.R. Matthews, "Tunable narrow line external cavity lasers for coherent optical systems," *Brit. Telecom. Tech. J.* **3**, 5-12 (1985).

[4] W.V. Sorin and S.A. Newton, "Single-frequency output from a broadband-tunable external fiber-cavity laser," *Optics Lett.* **13**, 731-733 (1988).

[5] M. Mittelstein, Y. Arakawa, A. Larsson, and A. Yariv, "Second quantized state lasing of a current pumped single quantum well laser," *Appl. Phys. Lett.* **49**, 1689-1691 (1986).

[6] M. Mittelstein, D. Mehuys, A. Yariv, J.E. Ungar, and R. Sarfaty, "Broadband tunability of gain-flattened quantum well semiconductor lasers with an external grating," *Appl. Phys. Lett.* **54**, 1092-1094 (1989).

[7] D. Mehuys, M. Mittelstein, A. Yariv, R. Sarfaty, and J.E. Ungar, "Optimized Fabry-Perot (GaAl)As quantum well lasers tunable over 105 nm," *Electron. Lett.* **25**, 143-145 (1989).

[8] See, for example, E. Yablonovitch and E.O. Kane, "Band structure engineering of semiconductor lasers for optical communications," *Journ. of Lightwave Tech.* **6**, 1292-1299 (1988).

[9] L. Eng, T.R. Chen, S. Sanders, Y.H. Zhuang, B. Zhao, A. Yariv, and H. Morkoc, "Submilliampere threshold current pseudomorphic InGaAs/AlGaAs buried heterostructure quantum well lasers grown by MBE," *Appl. Phys. Lett.* **55**, 1378-1380 (1989).

[10] D.F. Welch, C. Schaus, S. Sun, P.L. Gourley, and W. Streifer, "Gain characteristics of strained QW lasers," submitted to Applied Physics Letters.